Noncompetitive Inhibition of 5-HT$_3$ Receptors by Citral, Linalool, and Eucalyptol Revealed by Nonlinear Mixed-Effects Modeling

Gavin E. Jarvis, Roseli Barbosa, and Andrew J. Thompson

Department of Physiology, Development and Neuroscience, University of Cambridge, Cambridge, United Kingdom (G.E.J.); Mestrado em Bioprospecção Molecular, Universidade Regional do Cariri, Crato, Brazil (R.B.); and Department of Pharmacology, Cambridge, United Kingdom (A.J.T.)

ABSTRACT

Citral, eucalyptol, and linalool are widely used as flavorings, fragrances, and cosmetics. Here, we examined their effects on electrophysiological and binding properties of human 5-HT$_3$ receptors expressed in *Xenopus* oocytes and human embryonic kidney 293 cells, respectively. Data were analyzed using non-linear mixed-effects modeling to account for random variance in the peak current response between oocytes. The oils caused an insurmountable inhibition of 5-HT–evoked currents (citral IC$_{50}$ = 120 μM; eucalyptol = 258 μM; linalool = 141 μM) and did not compete with fluorescently labeled granisetron, suggesting a noncompetitive mechanism of action. Inhibition was not use-dependent but required a 30-second preapplication. Compound washout caused a slow (~180 seconds) but complete recovery. Coapplication of the oils with bilobalide or diltiazem indicated they did not bind at the same locations as these channel blockers. Homology modeling and ligand docking predicted binding to a transmembrane cavity at the interface of adjacent subunits. Liquid chromatography coupled to mass spectrometry showed that an essential oil extracted from *Lippia alba* contained 75.9% citral. This inhibited expressed 5-HT$_3$ receptors (IC$_{50}$ = 45 μg ml^{-1}) and smooth muscle contractions in rat trachea (IC$_{50}$ = 200 μg ml^{-1}) and guinea pig ileum (IC$_{50}$ = 20 μg ml^{-1}), providing a possible mechanistic explanation for why this oil has been used to treat gastrointestinal and respiratory ailments. These results demonstrate that citral, eucalyptol, and linalool inhibit 5-HT$_3$ receptors, and their binding to a conserved cavity suggests a valuable target for novel allosteric modulators.

Introduction

The natural oils citral, eucalyptol, and linalool (Fig. 1) are widely used as scents and flavorings in pharmaceuticals, foods, and health care products. Related compounds are reported to have antioxidant, anti-inflammatory, antiproliferative, antimicrobial, and acaricide activities. They belong to the terpenoid class of molecules that contains both structurally complex (e.g., bilobalide and ginkgolide) and simple (e.g., thymol and menthol) compounds (Caputi and Aprea, 2011). Terpenoids have effects on a broad selection of both voltage-gated and ligand-gated ion channels, and some are noncompetitive ligands of 5-hydroxytryptamine 3 (5-HT$_3$) receptors (Hall et al., 2004; Ashoor et al., 2013; Kessler et al., 2014; Lansdell et al., 2015; Ziemba et al., 2015).

5-HT$_3$ receptors belong to the Cys-loop family of transmembrane ligand-gated ion channels, which are responsible for fast excitatory and inhibitory neurotransmission in the central and peripheral nervous systems. It includes vertebrate nicotinic acetylcholine, GABA and glycine receptors, invertebrate receptors such as the glutamate-gated chloride channel (GluCl) and resistance-to-dieldrin channels (RDL), and prokaryotic homologs such as *Erwinia* chrysanthemi ligand-gated ion channel (ELIC) and *Gloeobacter* violaceus ligand-gated ion channel (GLIC) (Thompson et al., 2010). Each channel comprises five subunits surrounding a central ion-conducting pore, and each subunit has three distinct domains referred to as extracellular, transmembrane, and intracellular. The orthosteric binding site (that occupied by endogenous agonist) is located in the extracellular domain at the interface of two adjacent subunits, where binding is coordinated by the convergence of six peptide loops (Hassaine et al., 2014). The transmembrane domain of each subunit contains four α-helices (M1–M4), with M2 from each forming a central ion-conducting pore; to aid comparisons of the channel-lining residues of M2 from different Cys-loop receptors, a prime notation is often used to define residue positions, with 0' representing a conserved charged residue at the cytoplasmic side of the membrane. The intracellular domain regulates receptor trafficking, intracellular modulation, and ion channel conductance, but remains structurally unresolved (Hassaine et al., 2014).

5-HT$_3$ receptor ligands typically target extracellular and transmembrane domains. Competitive antagonists such as granisetron

ABBREVIATIONS: BB, bilobalide; DMEM, Dulbecco's modified Eagle's medium; DTZ, diltiazem; ELIC, *Erwinia* chrysanthemi ligand-gated ion channel; G-FL, granisetron-fluorescein; GLIC, Gloeobacter violaceus ligand-gated ion channel; GluCl, glutamate-gated chloride channel; HEK293, human embryonic kidney 293; LC-MS, gas-liquid chromatography coupled to mass spectrometry; OELa, essential oil extracts from *Lippia alba*; PRED, predicted agonist-induced response; RDL, resistance-to-dieldrin channels; RUV, residual unexplained variance.
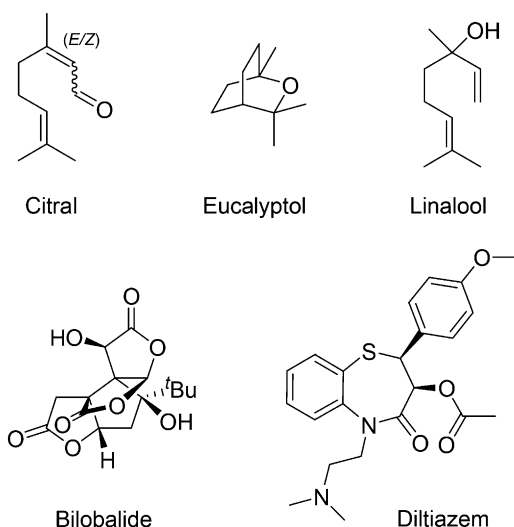
Fig. 1. Chemical structures of diltiazem and the terpenoids used in this study.

and tropisetron are used in the clinic to alleviate nausea and vomiting associated with chemotherapy, radiotherapy, and general anesthesia. There has also been limited use of partial agonists and competitive antagonists in the management of irritable bowel syndrome (Moore et al., 2013). Allosteric ligands include the anthelmintic ivermectin and general anesthetic propofol, both of which bind to cavities in the transmembrane domain of vertebrate, invertebrate, and prokaryotic channels (Nury et al., 2011; Chiara et al., 2013; Jayakar et al., 2013; Yip et al., 2013). Smaller terpenoids such as menthol and thymol also bind in transmembrane cavities, whereas more complex terpenoids such as bilobalide and ginkgolide bind in the channel of the 5-HT₃ receptor and other Cys-loop receptors (Hawthorne et al., 2006; Thompson et al., 2010; Lynagh and Lynch, 2012; Lynagh and Laube, 2014).

Medicinal products containing terpenoids are widely available for the relief of gastrointestinal and respiratory disorders. Although the pharmacological mechanisms of their active ingredients are not well known, evidence suggests the actions of some may result from effects at 5-HT₃ receptors. For example, menthol has an IC_{50} of 163 μM at 5-HT₃ receptors and blocks gut contractions at the same concentration (Heimes et al., 2011; Ashoor et al., 2013). The ginger extracts 6-gingerol and 6-shogaol similarly inhibit 5-HT₃ receptors and 5-HT–mediated gut contractions with micromolar potency (Abdel-Aziz et al., 2006; Walstab et al., 2013, 2014). With an increasing number of reports also describing the effects of terpenoids at other receptors, the potential physiologic effects of these compounds deserve investigation (Oz et al., 2015).

In this study, we investigate the pharmacology of the terpenoids citral, linalool, and eucalyptol. We use nonlinear mixed-effects modeling to determine their effects on the electrophysiology of 5-HT₃ receptors and, combined with flow cytometry and in silico docking, investigate their modes of action and potential binding sites. Using liquid chromatography coupled to mass spectrometry (LC-MS), we also report the terpenoid content of an essential oil extracted from *Lippia alba* and determine its effects on the contraction of isolated ileum and trachea.

Materials and Methods

Materials. Citral, eucalyptol, linalool (Fig. 1), and 5-hydroxytryptamine were from Sigma-Aldrich (St. Louis, MO). Human 5-HT3A (accession number: P46098) subunit cDNA was provided by J. Peters (University of Dundee, Dundee, UK). Essential oil of *L. alba* was purchased and a species voucher was deposited on Prisco Bezerra Herbarium (Federal University of Ceará, Ceará, Brazil) with the following number identification: EAC-08474. Essential oil extracts from *L. alba* (OELa) were analyzed by LC-MS at Parque de Desenvolvimento Tecnológico (Ceara, Brazil).

Oocyte Maintenance. Oocytes from *Xenopus laevis* were purchased from EcoCyte Bioscience (Castrop-Rauxel, Germany) and stored at 16°C in ND96 (96 mM NaCl, 2 mM KCl, 1 mM MgCl₂, 5 mM HEPES, pH 7.5).

Cell Culture. Human embryonic kidney 293 (HEK293) cells were grown on 90-mm round tissue culture plates as monolayers in Dulbecco's modified Eagle's medium (DMEM)/F12 (Gibco, Life Technologies, Carlsbad, CA) supplemented with 10% fetal bovine serum (Sigma-Aldrich) at 37°C in a moist atmosphere containing 5% CO₂.

Receptor Expression. 5-HT3A subunit cDNA was cloned into pGEMHE for oocyte expression. cRNA was transcribed in vitro from a linearized plasmid cDNA template using the mMessage mMachine Ultra T7 Transcription kit (Ambion, Austin, TX). Stage V and VI oocytes were injected with 50 nl of 100–500 ng μl⁻¹ cRNA (5–25 ng injected), and currents were recorded 1–4 days postinjection.

5-HT3A subunit cDNA was cloned into pcDNA3.1 for expression in HEK293 cells (ThermoFisher Scientific, Waltham, MA). Cells were transiently transfected with this cDNA using polyethyleneimine (25 kDa, linear, powder; Polysciences Inc., Eppelheim, Germany). Thirty microliters of polyethyleneimine (1 mg ml⁻¹), 5 μg of cDNA, and 1 ml of DMEM were incubated for 10 minutes at room temperature, added dropwise to a 90-mm plate of 70–80% confluent HEK293 cells, and incubated for 2–3 days before use.

Electrophysiology. Using two-electrode voltage clamp, *Xenopus* oocytes were routinely clamped at −60 mV using an OC-725 amplifier (Warner Instruments, Hamden, CT), NI USB-6341 X Series DAQ Device (National Instruments, Berkshire, UK), and the Strathclyde Electrophysiology Software Package v4.7.3 (University of Strathclyde, Glasgow, UK). Microelectrodes were fabricated from borosilicate glass (GC120TF-10; Harvard Apparatus, Edenbridge, Kent, UK) using a two-stage horizontal pull (P-97; Sutter Instrument Company, Novato, CA) and filled with 3 M KCl. Pipette resistances ranged from 0.8 to 2.0 MΩ. Oocytes were placed in a perfusion chamber made from 2-mm-wide × 30-mm-long silicon tubing that was cut in half lengthways (total volume ∼0.1 ml), and were perfused with ND96 at a rate of 12 ml min⁻¹. Drug application was via a simple gravity-fed system calibrated to run at the same rate. For inhibition measurements, antagonists were routinely applied for 1 minute before coapplication with 5-HT. A 3-minute wash was used between compound applications. Oils were dissolved in buffer containing 1% DMSO, freshly prepared each day, and constantly stirred during the experiments.

Flow Cytometry. HEK293 cells expressing the 5-HT₃ receptor were grown in monolayers and harvested from a 90-mm culture dish using 10 ml of Trypsin-EDTA (Sigma-Aldrich) for 10 minutes at 37°C. Digestion was terminated by the addition of 25 ml DMEM + 10% fetal bovine serum, and cells were pelleted at low speed for 2 minutes. The pellet was resuspended in 3 ml of phosphate-buffered saline (137 mM NaCl, 8.0 mM Na₂HPO₄, 2.7 mM KCl, 1.47 mM KH₂PO₄, pH 7.4), and cells were filtered through a cell strainer (BD Falcon, Franklin Lakes, NJ). Competition binding was measured by incubating HEK293 cells with different concentrations of nonlabeled ligands and 10 nM fluorescent granisetron (G-FL). After 10-minute incubation, cells were pelleted and rapidly washed in phosphate-buffered saline before being resuspended in the same buffer and analyzed on a BD Accuri C6 flow cytometer (Becton, Dickinson and Company, Franklin Lakes, NJ) at 488-nm excitation/530-nm emission. The geometric mean was measured at each concentration of test compound and fitted to eq. 1 (see

the following section) using a least-squares method (GraphPad Prism v4; GraphPad Software, La Jolla, CA).

Nonlinear Mixed-Effects Modeling. Inhibition of 5-HT–induced currents was analyzed using Wings for NONMEM (distributed under a GNU General Public License) and NONMEM 7.3.0 (Icon PLC, Dublin, Ireland). NONMEM is typically used for population pharmacokinetic/pharmacodynamic analyses and is ideally suited to simultaneously model fixed nonlinear effects (e.g., drug concentration-response relationships) and random effects (e.g., variance in maximal peak current). Nonlinear mixed-effects modeling of this sort cannot easily be done using more familiar statistical packages. Specifically, NONMEM allows the modeling of the relationship between drug and response, and importantly, the random between-oocyte variance, which is considerable. NONMEM enabled a single unified model to be created that included all electro-physiological agonist and antagonist data. This comprised 532 individual data points from 55 oocytes from the following experiments: 1) control 5-HT concentration-response data, 2) 5-HT concentration-response data in the presence of test compounds, and 3) concentration-inhibition data at fixed 5-HT (typically 1.7 μM) concentrations. The ability to allow for between-oocyte variance enabled raw peak currents to be analyzed, rather than normalized values. Normalization can obscure relationships between parameters, resulting in inaccurate and imprecise estimates of drug effects. Differences in peak currents and agonist potency between different oocytes were modeled with population variances (ω^2) associated with model parameters.

A structural model defined the relationship between the independent variables (i.e., agonist and antagonist concentrations) and the peak current (dependent variable). The agonist response was modeled using the four-parameter logistic equation:

$$PRED = \frac{Min_0 - Max_0}{\left(1 + \left([A]/10^{-pEC_{50,0}}\right)^{n_{H(A)}}\right)} + Max_0 \quad (1)$$

where PRED = predicted agonist-induced response, [A] = agonist concentration; Min_0 = PRED when [A] = 0; Max_0 = PRED when [A] = ∞; $pEC_{50,0}$ = $-\log_{10}[A]$ that induces PRED = ($Max_0 + Min_0$)/2; and $n_{H(A)}$ = agonist Hill coefficient. (In all cases, there was no basal current; hence, Min_0 was fixed to zero.)

Current responses can change during an experiment. If this effect is not identified and quantified, it can distort estimates of agonist and compound effects. The effect of time on the agonist response was modeled linearly as:

$$Max_T = Max_0(1 + (T \times n_T)) \quad (2)$$

where Max_0 = as in eq. 1; Max_T = PRED when [A] = ∞ at time T; T = time (hours) from start of individual experiment; and n_T = change in response per hour expressed as a proportion of the response at T = 0 (n_T = 0 represents no change; n_T = −0.1 represents a reduction of 10%, and n_T = 0.1 represents an increase of 10% per hour).

The effect of the compounds on Max_T was modeled as follows:

$$Max_{(D)} = \frac{Max_T}{\left(1 + \left([D]/10^{-pIC_{50}}\right)^{n_{H(D)}}\right)} \quad (3)$$

where Max_T = PRED when [A] = ∞ in the absence of drug D at time T (eq. 2); $Max_{(D)}$ = PRED when [A] = ∞ in the presence of drug D at time T; [D] = concentration of inhibitor drug; pIC_{50} = $-\log_{10}[D]$ in the presence of which $Max_{(D)}$ = $Max_T/2$; and $n_{H(D)}$ = inhibitor Hill coefficient. (This model assumes that, when [D] = ∞, PRED = 0.)

The effect of the compounds on agonist pEC_{50} was modeled as follows:

$$pEC_{50(D)} = pEC_{50,0} - n_{G(D)}\left[\log_{10}\left([D]/10^{-pA_{2(D)}}\right)^{n_{S(D)}} + 1\right] \quad (4)$$

where: $pEC_{50,0}$ = agonist pEC_{50} in the absence of drug D (eq. 1); $pEC_{50(D)}$ = agonist pEC_{50} in the presence of drug D; [D] = concentration

of drug; $pA_{2(D)}$ = pA_2 of drug D; $n_{S(D)}$ = Schild coefficient for drug D; and $n_{G(D)}$ = inhibition coefficient for drug D.

Variable Schild (n_S) and inhibition (n_G) coefficients enabled compound effects other than competitive-like inhibition to be modeled, and hypotheses about drug action on pEC_{50} to be statistically evaluated using likelihood ratio tests. For example, when n_S = 1 and n_G = 1, the effect on agonist pEC_{50} is consistent with that of a competitive antagonist, and when n_G = 0, there is no effect of the drug on agonist pEC_{50}.

Random effects (η) were included, enabling parameter values from different oocytes to differ from the typical, population parameter estimates. The relationship between population and individual oocyte parameters was modeled in the following two ways:

$$Par_{IND} = Par_{POP} \times e^{\eta_i} \quad (5)$$

$$Par_{IND} = Par_{POP} + \eta_i \quad (6)$$

where Par_{IND} = individual parameter estimate; Par_{POP} = population parameter estimate; and η_i = η value representing the difference between the population and an individual (i) parameter estimate. Values of η from all oocytes (n = 55) enabled a variance-covariance (OMEGA) matrix for random effects to be constructed. This allows the random variance inherent in different oocytes to be defined and correlations in estimated parameters to be identified.

Residual unexplained variance (RUV) defines the difference between the observed and predicted values for a given set of conditions. RUV was modeled as a function of PRED as follows:

$$RUV = \alpha^2 \times PRED^{\gamma} \quad (7)$$

where RUV = residual unexplained variance between observed and predicted current; PRED = predicted current; α^2 = variance parameter; and γ = variance scaling parameter. When γ = 0, RUV is constant irrespective of PRED and α = standard deviation of the residual variability; when γ = 1, RUV is proportional to the response (α^2 = RUV/PRED); when γ = 2, the coefficient of variation of the residual variability is constant (α = SD_{RESID}/PRED).

Maximum likelihood was used to identify best fit parameters for specific models. A Laplacian method was used to obtain parameter estimates. The objective function used by NONMEM is the extended least squares. Parameter standard errors are from the covariance step in NONMEM. Models were evaluated by examining both population- and individual-weighted residuals and comparing Akaike and Bayesian information criteria. Specific hypothesis tests are defined in Table 1. They were performed by constraining parameters and comparing resultant differences in extended least squares values using likelihood ratio tests (Spalding and Jarvis, 2002; Mould and Upton, 2013).

Drug Effects at 5-HT$_{3}$A$_{T6'S}$ Receptors. The effects of the compounds on 5-HT$_{3}$A$_{T6'S}$ receptors were also evaluated. A total of 113 data values from 11 oocytes comprising control 5-HT concentration-response and compound concentration-inhibition curves were incorporated into the wild-type receptor data set. Parameters were incorporated into the model that defined changes in pEC_{50}, pIC_{50}, Max_0, and pA_2 values for 5-HT$_{3}$A$_{T6'S}$ receptors. These parameters were statistically evaluated as described earlier.

Dual Application. Dual application studies were performed as previously described (Jarvis and Thompson, 2013). This is a simple method to determine whether two channel blockers share the same binding site (syntopic inhibition) or bind to separate locations (allotopic inhibition). For each test compound, inhibition of a supramaximal 5-HT–induced (100 μM) response was measured alone and in combination with bilobalide (BB) and diltiazem (DTZ), both well characterized 5-HT$_3$ blockers (Fig. 1; Thompson et al., 2011a). Concentrations of the test compounds, BB and DTZ, were selected such that they caused approximately 62% inhibition when used alone. From the results of these experiments, predicted levels of inhibition were derived for both

TABLE 1
Output from the best fit model describing the effects of 5-HT and inhibitors on the peak current
The best fit was selected based the stability of convergence on the objective function (extended least squares = 110.89) and a comparison of Akaike information criteria (1,132.64) and Bayesian information criteria (1,226.72) values to alternative models. The model was further evaluated by examining the relationship between observed and predicted values, and population and individual residuals.

Parameter	Population Parameter Estimate	Population Variance Model	Population SD(ω) or CORR[b]	Hypothesis Tests	P Value (LRT)	Interpretation
Agonist (5-HT)						
Min (μA)	0 (fixed)	—	—	—	—	
Max (μA)	4.94 ± 0.64	$\times$ EXP(η_2)	0.95 ± 0.10	H$_0$: $\omega_{2,2}$=0	No result[a]	Max varies between oocytes
COV(η_1,η_2)			0.87 ± 0.05	H$_0$: $\omega_{1,2}$=0	4×10^{-9}	Max and pEC$_{50}$ correlate strongly
pEC$_{50}$	5.65 ± 0.03	+ η_1	0.18 ± 0.02	H$_0$: $\omega_{1,1}$=0	4×10^{-35}	pEC$_{50}$ varies between oocytes
n_H	2.94 ± 0.13			H$_0$: $n_{H(A)}$=3	0.64	Suggests three highly cooperative agonist binding sites
n_T	-0.13 ± 0.06	+ η_7	0.19 ± 0.06	H$_0$: n_T=0	0.052	Weak evidence for a change in response with time
				H$_0$: ω_7=0	0.004	n_T varies between oocytes
Citral						
pIC$_{50}$	3.92 ± 0.05	+ η_5	0.16 ± 0.04	H$_0$: ω_5=0	2×10^{-11}	pIC$_{50}$ varies between oocytes
n_H	1.34 ± 0.08			H$_0$: n_H=1	5×10^{-6}	Indication of cooperative binding
n_G	0 (fixed)			H$_1$: $\{n_G,pA_2,n_S\}$≠0	0.94	No evidence that citral changes agonist pEC$_{50}$
Eucalyptol						
pIC$_{50}$	3.59 ± 0.11	+ η_4	0.32 ± 0.07	H$_0$: ω_4=0	1×10^{-16}	pIC$_{50}$ varies between oocytes
n_H	1.04 ± 0.11			H$_0$: n_H=1	0.76	Suggests one inhibitor binding site
n_G	1 (fixed)			H$_0$: n_G=0	4×10^{-15}	Strong evidence that eucalyptol changes agonist pEC$_{50}$
pA$_2$	3.09 ± 0.09	+ η_3	0.18 ± 0.06	H$_0$: ω_3=0	0.006	pA$_2$ varies between oocytes
n_S	1.70 ± 0.24			H$_0$: n_S=1	0.001	Schild slope greater than that for competitive antagonism
Linalool						
pIC$_{50}$	3.85 ± 0.02	+ η_6	0.05 ± 0.02	H$_0$: ω_6=0	0.023	pIC$_{50}$ varies between oocytes
n_H	2.19 ± 0.26			H$_0$: n_H=2	0.46	Suggests two highly cooperative inhibitor binding sites
n_G	0 (fixed)			H$_1$: $\{n_G,pA_2,n_S\}$≠0	0.11	No/weak evidence that linalool changes agonist pEC$_{50}$
RUV model						
γ	1.30 ± 0.07			H$_0$: γ=0	1×10^{-63}	Residual error variance increases with the current amplitude
α	0.30 ± 0.01					

COV, covariance; LRT, likelihood ratio test.
[a]No stable convergence was obtained without a random effect included.
[b]Parameter estimates are shown $\pm$ standard errors.

allotopic and syntopic modes of action. These predictions were compared with data obtained experimentally using the same concentrations of the inhibitors acting together. For each oocyte, the change in the amplitude of the 5-HT response over time was monitored and taken into account. Inhibition by drugs was quantified in relation to interpolated control responses for each time point.

The dual application measurements were compared statistically with allotopic and syntopic predictions using a two-way analysis of variance in which the oocyte was included as a random effect (SPSS Statistics 20; IBM, Armonk, NY). Post-hoc testing was with Dunnett's method, comparing the measured data to each of the predictions.

Modeling and Ligand Docking. Using ClustalW (EMBL-EBI, Cambridge, UK), the protein sequence of the human 5-HT3A subunit (accession: P46098) was aligned with the sequence from the mouse 5-HT$_3$A crystal structure (Protein Data Bank ID: 4PIR). Sequence identity between mouse and human 5-HT$_3$A was 89.1% (EMBOSS Needle; EMBL-EBI; McWilliam et al., 2013) and alignments were unambiguous. Five pentameric homology models were generated using Modeler 9.13 (Andrej Sali, San Francisco, CA) with default parameters, and the best model was selected using Ramachandran plot analysis. Citral, eucalyptol, and linalool were constructed ab initio in Chem3D Ultra 7.0 (CambridgeSoft, Cambridge, UK) and energy minimized using the MM2 force field. Potential binding sites were identified using a 20-Å docking sphere centered on the α-carbon of L320, a residue located within the center of M2; therefore, within each subunit, the docking sphere encompassed the full length of all transmembrane α-helices. Docked poses were generated using the GOLD docking program (version 3.0; Cambridge Crystallographic Data Centre, Cambridge, UK) with the GOLDScore function and default settings. For each compound, 10 docking poses were generated, and the poses and predicted hydrogen bonds were visualized with PyMol v1.3 (Schrödinger, New York, NY).

Ileum Preparation. Guinea pig ileum was obtained from adult male guinea pigs (200–300 g). The ileum was cut into 1-cm lengths and mounted longitudinally to a force transducer with a resting tension of 0.5 g in a 10-ml water-jacketed organ bath containing Krebs' buffer (118 mM NaCl, 4.7 mM KCl, 1.2 mM MgSO$_4$, 1.25 mM CaCl$_2$, 11 mM glucose, 10 mM HEPES, pH 7.2) continuously aerated with 95% O$_2$/5% CO$_2$ and kept at 37°C. The ileum segments were allowed to equilibrate for 10 minutes before the experiments were started, and contractile responses were recorded using LabChart 6 (ADInstruments Ltd., Oxford, UK). 5-HT was applied to the serosal layer of the ileum, and contractions were recorded for 10 seconds. Following drug applications, the organ bath was flushed twice with fresh Krebs' solution, and the ileum was allowed to recover for 10 minutes prior to the next application. Antagonist was preapplied for 10 minutes before coapplying 5-HT. Application of antagonists was not undertaken until two similar (± 5%) 5-HT contractions were recorded in the absence of antagonist. Experiments involving animals were approved by the University of Cambridge Animal Welfare and Ethical Review Body (reference: PHARM 004/15).

Tracheal Preparation. The trachea was removed from male Wistar albino rats (250–350 g), cut into 2-cm lengths, and mounted on a force transducer with a resting tension of 1.0 g in a 10-ml water-jacketed organ bath containing modified Tyrode's solution (136 mM NaCl, 5 mM KCl, 0.98 mM MgCl$_2$, 0.36 mM NaH$_2$PO$_4$, 2 mM CaCl$_2$,

11.9 mM NaHCO$_3$, 5.5 mM glucose, pH 7.4) continuously aerated with 95% O$_2$/5% CO$_2$ and kept at 37°C. Contractile responses were recorded using a force transducer (model FT03; Grass Technologies, Quincy, MA) connected to a PC-based data acquisition system (Dataq, PM-1000; DATAQ Instruments Inc., Akron, OH). The experiments were conducted after an equilibration period of 60 minutes and three successive similar contractile responses. Experiments were approved by the local animal ethics committee (protocol number 00084/2014.2).

Results

Effects of Citral, Eucalyptol, and Linalool on 5-HT$_3$ Receptor Currents. Neither 5-HT nor the terpenoid oils (Fig. 1) had observable effects on uninjected *Xenopus* oocytes. By contrast, application of 5-HT to *Xenopus* oocytes expressing 5-HT$_3$ receptors produced concentration-dependent, rapidly activating, inward currents that slowly desensitized (Fig. 2A). These responses were abolished by the 5-HT$_3$ receptor–selective antagonist granisetron (100 nM).

Citral, eucalyptol, and linalool inhibited 5-HT–evoked currents in oocytes expressing 5-HT$_3$ receptors in a concentration-dependent manner (Figs. 2 and 3) that was unaffected by the clamp potential (Fig. 2G), but had no effect when applied without 5-HT. Preapplication of the oils increased the level of inhibition of the 5-HT response. Figure 2B shows how simultaneous application of 5-HT and citral caused a small reduction in the 5-HT peak current with subsequent responses showing greater inhibition until a stable level of inhibition was achieved. This is also seen in Fig. 2F, where a plot of preapplication time against inhibition shows there was no further increase in the level of inhibition after 30-second preapplication for all three compounds.

Following removal of the compounds, full recovery of 5-HT responses took approximately 3 minutes. This was independent of the frequency of 5-HT application during the recovery period, as shown for citral in Fig. 2C. The rate of recovery from inhibition was similar whether the compounds were applied in the absence of (Fig. 2D, top), immediately prior to (Fig. 2D, middle), or during (Fig. 2D, bottom) 5-HT application. The slow recovery from inhibition was also seen when the three compounds were added and removed in the continuous presence of 5-HT, as no rebound currents were seen, unlike the more rapidly recovering channel blocker diltiazem (Fig. 2E).

These results show that citral, eucalyptol, and linalool inhibit 5-HT$_3$ receptors and defined the conditions for subsequent experiments.

Quantification and Mechanism of Block. Studies at varying 5-HT (0.3–300 μM), citral (10, 30, 100, 200, 300, 500, 600, and 1000 μM), eucalyptol (100, 200, 500, 660, and 2000 μM), and linalool (100, 200, 500 μM) concentrations were carried out at −60 mV with a 30-second preapplication of oils and a 3-minute washout.

Peak current responses were reproducible within oocytes but varied substantially between oocytes. A total of 532 peak current values from 55 oocytes were analyzed using nonlinear mixed-effects modeling to characterize and quantify the effects of the compounds. The model included parameters that defined concentration-dependent inhibitor effects on the maximum response (Max$_0$) and pEC$_{50}$ of 5-HT.

The results from the best fit model are graphically represented in Fig. 3, with the parameter values shown in Table 1, along with the outcome of hypothesis tests of these parameters.

Figure 4A shows a linear relationship between observed and predicted peak current values. The most parsimonious and stable variance-covariance model consisted of seven random effects (Table 1). The analysis with NONMEM also revealed a strong covariance between the maximum response (Max$_0$) and pEC$_{50}$ of 5-HT (Fig. 4B: correlation = 0.869 ± 0.054), indicating that oocytes with a higher peak current were more sensitive to 5-HT. Failure to account for this covariance, such as by normalizing data, misrepresents the variance in the responses and could lead to inaccurate conclusions about the effects of the inhibitors on 5-HT pEC$_{50}$ values. For example, the insets in Fig. 3 show normalized representations of the same data revealing apparent shifts in the EC$_{50}$ values for citral and linalool that were not evident when the covariance was taken into account. Furthermore, IC$_{50}$ values derived from these normalized data were lower (e.g., higher potency; citral = 98 μM; eucalyptol = 174 μM; linalool = 83 μM).

In the population of oocytes used ($n = 55$), the 5-HT pEC$_{50}$ was 5.65 ± 0.03 (EC$_{50}$ = 2.25 μM) with a Hill coefficient of 2.94 ± 0.13 (Table 1). This is similar to previous findings and is consistent with strong positive cooperativity between three agonist binding sites (Thompson et al., 2011a; Thompson and Lummis, 2013). Neither citral nor linalool altered the pEC$_{50}$ of 5-HT, but both caused a concentration-dependent reduction in the maximal peak current response (Fig. 3; Table 1). For citral, the pIC$_{50}$ was 3.92 ± 0.05 (IC$_{50}$ = 120 μM), and for linalool, 3.85 ± 0.02 (IC$_{50}$ = 141 μM). Eucalyptol also caused a reduction in the maximal peak current with a pIC$_{50}$ of 3.59 ± 0.11 (IC$_{50}$ = 258 μM), although this was accompanied by a reduction in the pEC$_{50}$ of 5-HT (Fig. 3; Table 1) with a pA_2 and apparent Schild coefficient (defining the shift in the agonist pEC$_{50}$) of 3.09 ± 0.09 and 1.70 ± 0.24, respectively.

These results are consistent with a simple noncompetitive mechanism of action for each compound, but suggest that eucalyptol may have additional effects.

Effects on a 5-HT$_{3}$A$_{T6'S}$ Receptor Mutant. Thymol and carvacrol activate human 5-HT$_3$ receptors from a transmembrane binding site (Lansdell et al., 2015). The compounds studied here are structurally similar and could have weak partial agonist activities that are difficult to detect at wild-type receptors. The agonist sensitivity of the 5-HT$_3$ receptor can be enhanced by a T6'S substitution in the pore-lining M2 α-helix of the 5-HT$_3$A subunit (Thompson and Lummis, 2013). We therefore investigated the effects of 5-HT and the terpenoid oils in oocytes expressing the 5-HT$_{3}$A$_{T6'S}$ mutant. A total of 112 peak current responses from 11 different oocytes were appended to the wild-type data set. These experiments comprised control 5-HT concentration-response data and concentration-inhibition data for 2 μM 5-HT. Parameters were included in the model that allowed differences in agonist and inhibitory effects to be quantified and evaluated.

There was no difference in the maximum 5-HT peak current in the wild-type and 5-HT$_{3}$A$_{T6'S}$ receptors [Max$_{0(T6'S)}$/Max$_{0(WT)}$ = 0.98 ± 0.30; $P = 0.93$], but the mutant was more sensitive to agonist as previously reported (Thompson and Lummis, 2013). The 5-HT pEC$_{50}$ was increased by 0.35 ± 0.07. Unlike the effects at wild-type receptors, eucalyptol did not alter the 5-HT pEC$_{50}$ [H$_0$: $n_{G(EUC/T6'S)} = 0$; $P = 0.71$]. When applied alone, citral, eucalyptol, and linalool did not evoke currents in the 5-HT$_{3}$A$_{T6'S}$ receptor mutant, but all abolished 5-HT–induced responses with inhibitory potencies that were
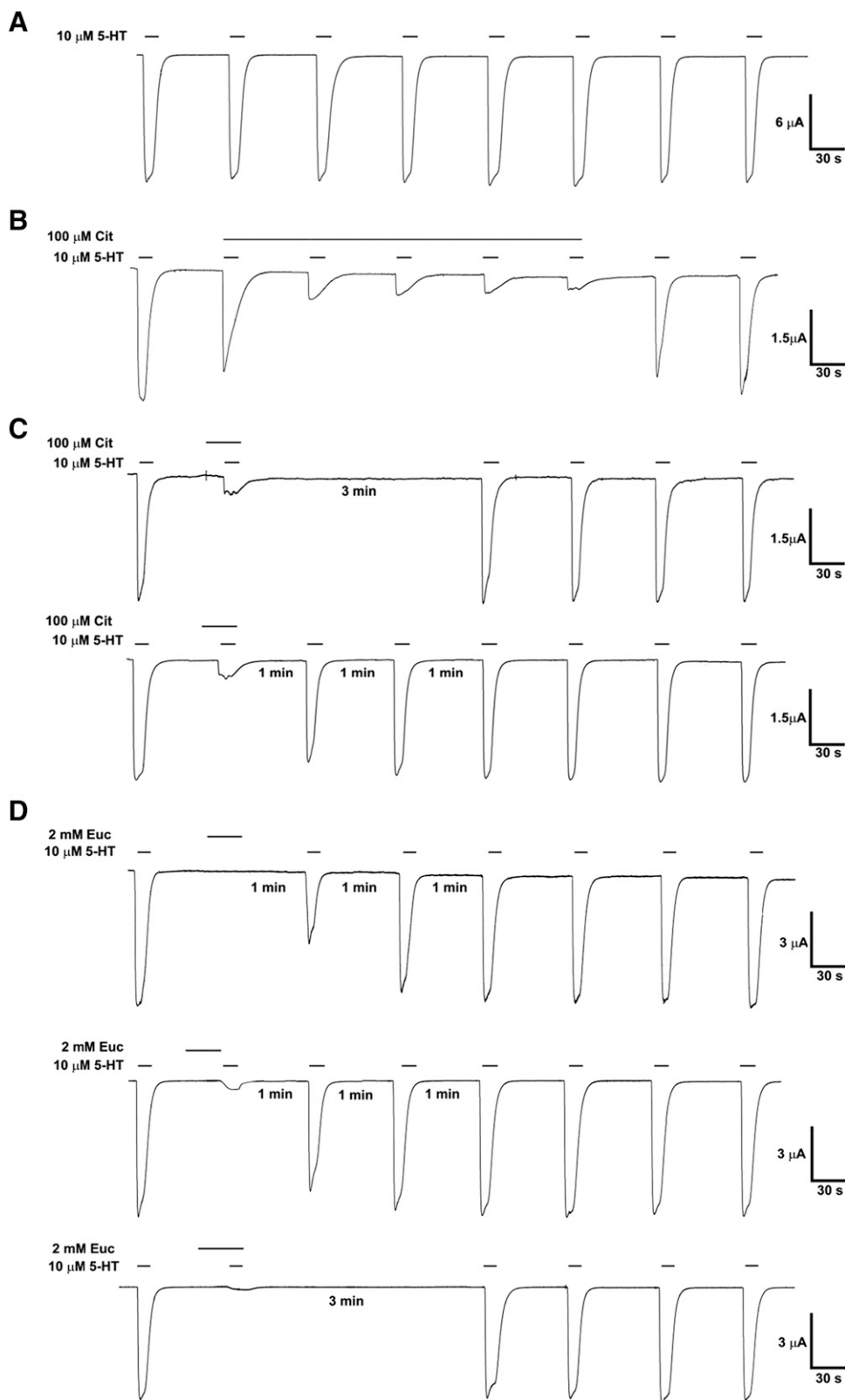
Fig. 2. Electrophysiological characterization of the actions of citral (Cit), eucalyptol (Euc), and linalool (Lin) at 5-HT$_3$ receptors. (A) Stable currents could be evoked by 10 μM 5-HT applied at 1-minute intervals. (B) At 10 μM 5-HT, stable levels of inhibition by citral, eucalyptol, or linalool were only seen following preapplication but remained stable thereafter [also see (F)]. (C) Following inhibition, responses were slow to recover. For all three compounds, full recovery was achieved after 3 minutes and was independent of the frequency of 5-HT activation during the recovery period. (D) Receptors were inhibited in the closed state as shown by the comparable levels of inhibition seen when the compounds were applied in the absence of 5-HT or during 5-HT application. Inhibition persisted after washout, and the recovery time was unaltered by the timing or frequency of subsequent 5-HT applications. (E) The slow washout of the compounds is highlighted by the absence of a rebound current following the removal of citral, eucalyptol, or linalool. By contrast, rebound was clearly seen following the removal of diltiazem, a channel blocker with faster recovery from inhibition. (F) At a concentration of 300 μM, the oils required 30-second preapplication to stably inhibit the 10 μM 5-HT response. At lower concentrations, the effect of preapplication was less apparent, since the 5-HT response took longer to reach a stable peak current. (G) The level of inhibition at +40 mV or −60 mV was the same for all three compounds.

reduced by approximately 2-fold when compared with their effects at wild-type receptors (Table 2).

Competitive Binding with Granisetron. Our analysis provides no evidence that citral or linalool competes with 5-HT at the orthosteric site, whereas the effect of eucalyptol on 5-HT

pEC$_{50}$ suggests that this ligand might. To further test for orthosteric interactions, we measured the binding of a fluorescent granisetron derivative (G-FL) together with the three compounds using flow cytometry (Jack et al., 2015). Both 5-HT and granisetron reduced G-FL binding in a
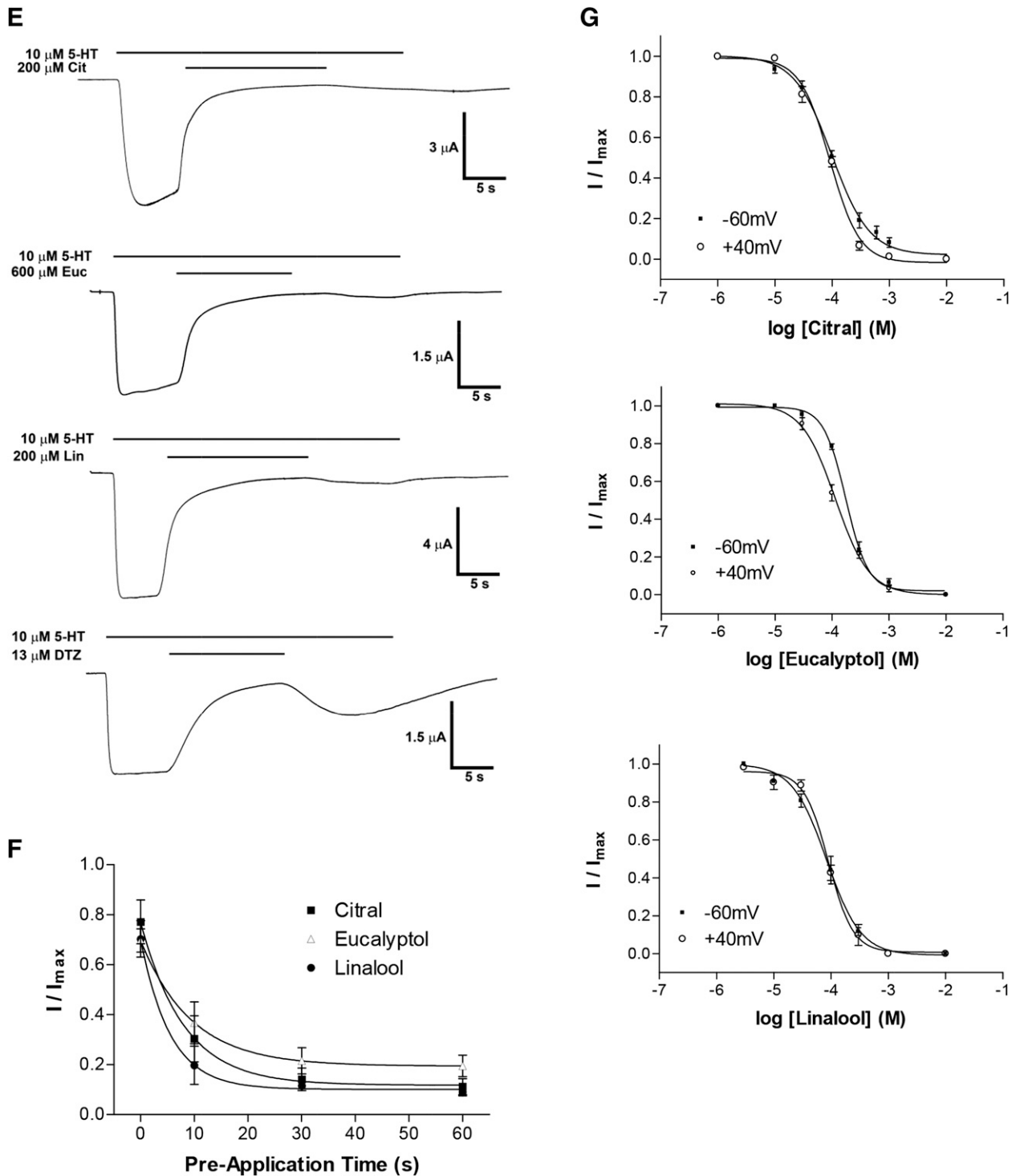
E

F

G

Fig. 2. Continued

concentration-dependent manner (Fig. 5A). Binding of G-FL was unaffected by citral, eucalyptol, or linalool at concentrations up to 1 mM (Fig. 5B).

Dual Application of Citral, Eucalyptol, or Linalool in the Presence of Bilobalide or Diltiazem. We have previously shown that simultaneous application of two drugs can be used to probe the sites of action of channel blockers (Jarvis and Thompson, 2013). Here, we applied each of the oils in the presence of bilobalide or diltiazem, channel-blocking antagonists that bind at the 2'-6' and 7' regions of the 5-HT$_3$ receptor pore, respectively (Thompson et al., 2011a).

For citral (Fig. 6A), measured dual inhibition was no different from the allotopic predictions for bilobalide ($P = 0.95$) or diltiazem ($P = 0.42$), but was greater than the syntopic predictions (BB, $P = 0.031$; DTZ, $P = 0.0004$). For eucalyptol (Fig. 6B), dual inhibition was similar to the allotopic
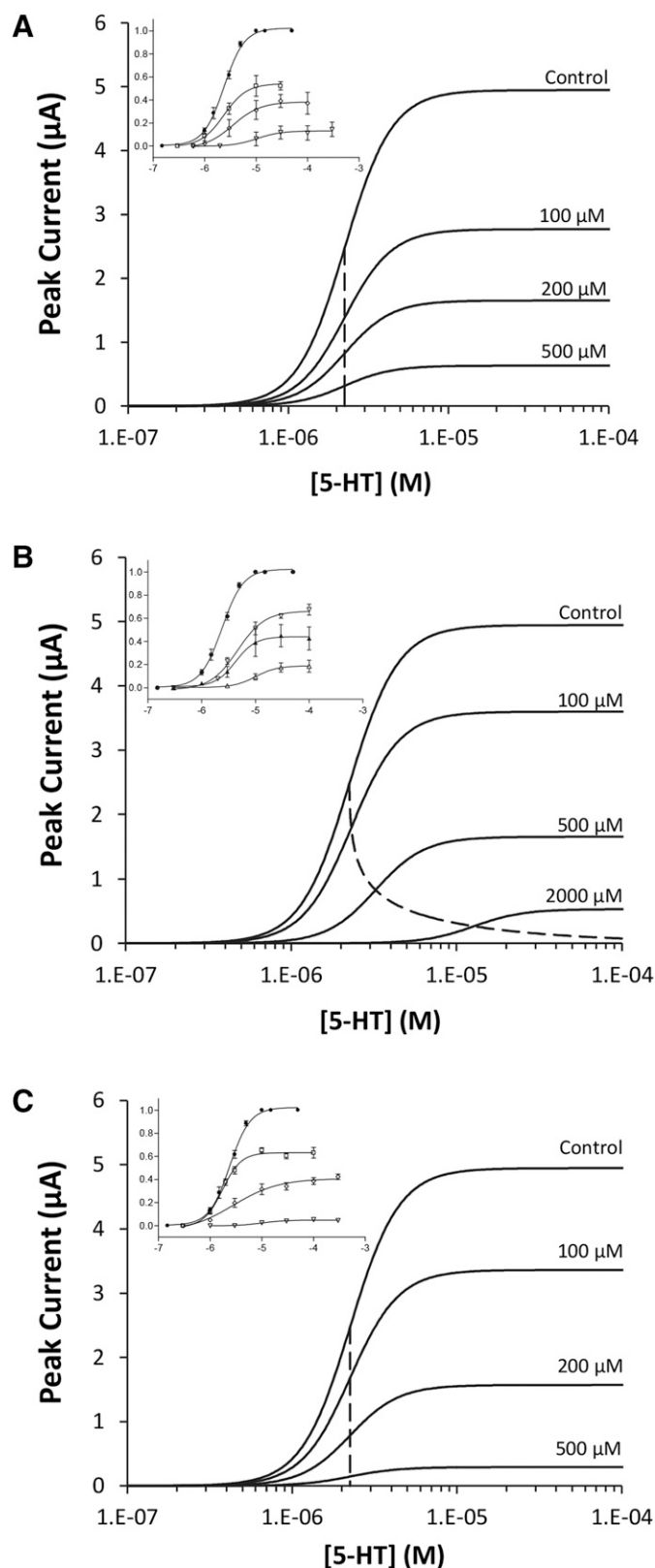
Fig. 3. Inhibition of the 5-HT$_3$ receptor by citral, eucalyptol, or linalool. 5-HT–induced currents were measured at −60 mV in the absence or presence of various concentrations of citral (A), eucalyptol (B), or linalool (C) following a 30-second preapplication. The data were analyzed as described in the text, and the output of this nonlinear mixed-effects modeling is shown in Table 1. The main features of the structural model are illustrated here. The dotted lines show the effect of the compounds on the EC$_{50}$. The insets show normalized data at the same inhibitor concentrations; for citral and linalool, the apparent shifts in the EC$_{50}$ seen in this normalized data are artifacts caused by the normalization. Additional data at 10, 30, 300, 600, and 1000 μM citral and 200 and 660 μM eucalyptol were also collected, but the curves are omitted for clarity.
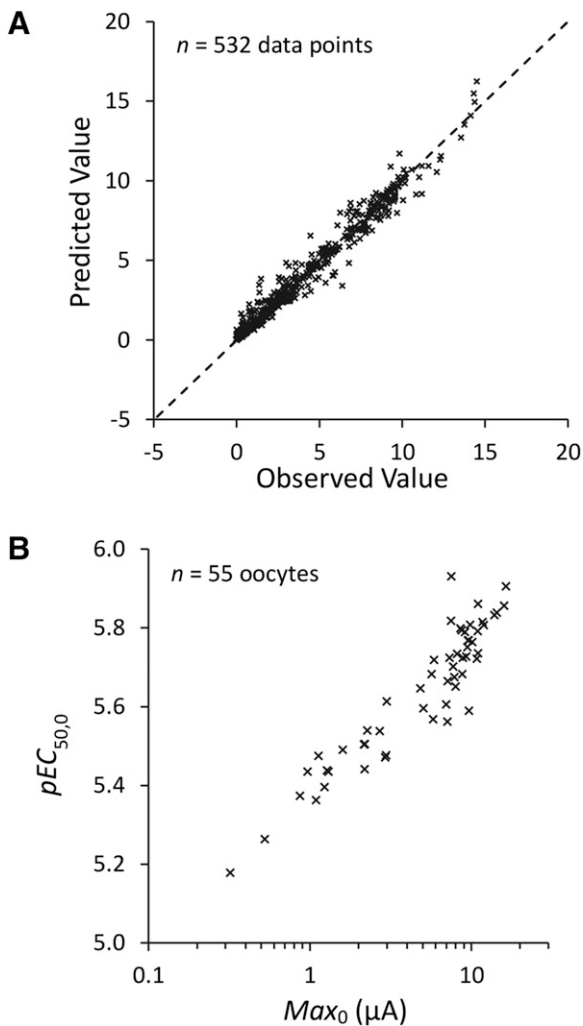
prediction for bilobalide ($P = 0.38$) but greater than the allotopic prediction for diltiazem ($P = 0.013$). For linalool (Fig. 6C), dual inhibition was greater than the allotopic prediction for both bilobalide ($P = 0.02$) and diltiazem ($P = 0.06$).

These results suggest that citral, eucalyptol, and linalool do not share binding sites with the channel blockers bilobalide or diltiazem, but may enhance their effects.

Transmembrane Binding Sites. Given the lipophilicity of the oils and their noncompetitive mechanism of action, we sought to identify potential binding sites in the transmembrane domain using in silico ligand docking in a homology model of the human 5-HT$_3$ receptor. Using a loosely defined binding site radius of 20 Å that encompassed the whole of the transmembrane domain, the major binding cavity for all of the ligands was predicted to be at the interface of two adjacent subunits, between M1-M2 of the principal subunit and M2-M3 of the complementary subunit. For linalool, all 10 docked poses were similarly orientated at the intersubunit interface within only a 2.29-Å root-mean-square deviation (Fig. 7A). Eucalyptol docked at two locations, both of which were clustered at the same site between two adjacent subunits (Fig. 7B). For citral, two sites were predicted, with the major docked pose cluster (6/10) at the same intersubunit cavity, and a minor site (4/10) at the lipid-exposed intracellular interface of the M1 and M4 α-helices (Fig. 7C). Linalool was the only compound predicted to make hydrogen bond contacts with the protein (in 4/10 docked poses), which were between the hydroxyl of linalool and the backbone carbonyl of Thr6' in M2 (Fig. 7D).

These results suggest that all three compounds could bind to a transmembrane cavity located at the interface of adjacent subunits.

Physiologic Effects. *L. alba* is used medicinally throughout Central and South America as a means of alleviating gastrointestinal discomfort and for respiratory ailments (Hennebelle et al., 2008). Here, we analyzed an OELa by LC-MS and detected that the main compounds were the terpenoids citral (75.9%; 41.8% geranial + 34.1% neral), 1-limoneno (9.8%), carvone (8.9%), gamma-terpinene (2.0%), and benzene [1-methyl-3-(1-methylethyl; 1.0%].

To determine whether the properties of this essential oil could be physiologically relevant, we measured its effects on 5-HT$_3$ receptors expressed in oocytes and on smooth muscle contractions in rat trachea and guinea pig ileum. At 5-HT$_3$ receptors expressed in oocytes, OELa had no effect when applied alone, but fully and reversibly inhibited the 2 μM 5-HT response with an IC$_{50}$ of 45 μg ml^{-1} ($n = 5$; Fig. 8A). In rat trachea, 5-HT-induced contractions were concentration-dependent and substantially inhibited by 10 μM of the 5-HT3 receptor antagonist granisetron (Fig. 8B). OELa also abolished contractions induced by 10 μM 5-HT with an IC$_{50}$ of 200 μg ml^{-1} (Fig. 8C). 5-HT–evoked contractions of guinea pig ileum were also inhibited by granisetron, and OELa had an IC$_{50}$ of 20 μg ml^{-1} ($n = 6$; Fig. 8D). In both rat trachea and

Fig. 4. Nonlinear mixed-effects modeling. (A) The relationship between observed and predicted peak current values for the best fit model described in Table 1 ($n = 532$). The values cluster around the line of unity with no apparent systematic deviation, showing that data are well fitted by the model. (B) Modeled Max_0 and $pEC_{50,0}$ parameter values for individual oocytes ($n = 55$ oocytes). The clear and strong relationship between these parameter estimates (correlation = 0.869 ± 0.054) suggests that oocytes with a high maximum peak current are more sensitive to 5-HT. This relationship is obscured by data normalization.

guinea pig ileum, recovery of contractions required extended washes, particularly at higher concentrations (Fig. 8E).

These results show that that OELa has a high citral content and inhibits 5-HT₃ receptors expressed in *Xenopus* oocytes and 5-HT–induced smooth muscle contraction in the trachea and ileum.

Discussion

This study describes the inhibitory effects of citral, eucalyptol, and linalool on human 5-HT₃ receptors. These terpenoids can be added to a growing list of structurally related compounds that modulate a wide range of voltage- and ligand-gated ion channels, including 5-HT₃ receptors and their related vertebrate, invertebrate, and prokaryotic homologs (Hales and Lambert, 1991; Barann et al., 2000; Hall et al., 2004; Garcia et al., 2006; Ashoor et al., 2013; Walstab et al., 2014; Lansdell et al., 2015; Ziemba et al., 2015).

TABLE 2

Effect of a T6'S mutation on inhibitor pIC_{50} values

Agonist	ΔpEC_{50}	P (H₀: ΔpEC_{50}=0)	$pEC_{50}{}^a$
5-HT	0.35 ± 0.07	3×10^{-6}	6.00 ± 0.08
Inhibitor[b]			
Citral	-0.36 ± 0.10	0.002	3.55 ± 0.11
Eucalyptol	-0.45 ± 0.22	0.046	3.14 ± 0.05
Linalool	-0.34 ± 0.04	5×10^{-7}	3.51 ± 0.24

[a]Standard errors were calculated from the errors of the pEC_{50}/pIC_{50} and $\Delta pEC_{50}/\Delta pIC_{50}$ values using propagation of error calculations.
[b]There was no significant difference between the ΔpIC_{50} values for the three inhibitors ($P = 0.87$).

All of the essential oils inhibited 5-HT–mediated currents with IC₅₀ values in the micromolar range. Non-competitive antagonism was shown by them causing a concentration-dependent reduction in the maximal 5-HT response and by not competing with the fluorescent antagonist G-FL. The Hill coefficients for the reduction in the 5-HT response suggested that there may be multiple binding sites with strong cooperativity for linalool ($n_H = 2.2$), weak cooperativity for citral ($n_H = 1.3$), and no cooperativity for eucalyptol ($n_H = 1.0$). There was evidence that, at higher concentrations, eucalyptol also caused a rightward shift in the EC₅₀ of 5-HT ($pA_2 = 3.09$), indicating an additional inhibitory mechanism. A competitive mechanism is conceivable, although not compelling, given that the shift had a Schild coefficient of 1.7 and that eucalyptol failed to compete with G-FL. However, given the different binding orientations of 5-HT and granisetron in cocrystal structures, it is possible that an inhibitor could compete with one of these ligands but not the other (Colquhoun, 2007; Kesters et al., 2013). At the T6'S mutants, there was no evidence of a eucalyptol-induced change in agonist EC₅₀. This is probably because this effect occurs at higher concentrations ($pA_2 = 3.09$) than the reduction in maximal current ($pIC_{50} = 3.59$), and the overall potency of the terpenoids was reduced at these mutants.

Mixed-effects modeling also revealed a strong correlation between the maximal peak current and pEC_{50} (Fig. 5B). Since receptor expression is difficult to control, many investigators normalize data to facilitate comparisons between experiments. However, if the implicit assumption that agonist response is independent of expression levels is not justified, then data normalization may lead to inaccurate and misleading conclusions. In the current study, a particular advantage of the nonlinear mixed-effects modeling was that variant maximal current responses could be modeled as a random effect, thereby generating more accurate quantitative conclusions (normalization yielded higher IC₅₀ values, suggesting that this method of analysis overestimated the potency of the compounds) and revealing unexpected biologic phenomena (such as the covariance of the EC₅₀ and Max_0). This modeling approach was also able to identify pleiotropic drug effects (e.g., eucalyptol), for which the properties of the compounds we used were particularly well suited. Therefore, the data we present clearly highlight the superior value of nonlinear mixed-effects modeling, revealing phenomena that would otherwise have been missed using the standard procedure of normalizing data. Nonlinear mixed-effects modeling is often used for pharmacokinetic-pharmacodynamic data analysis, but has broad applicability in other quantitative pharmacological studies (Mould and Upton, 2013). For example, by modeling
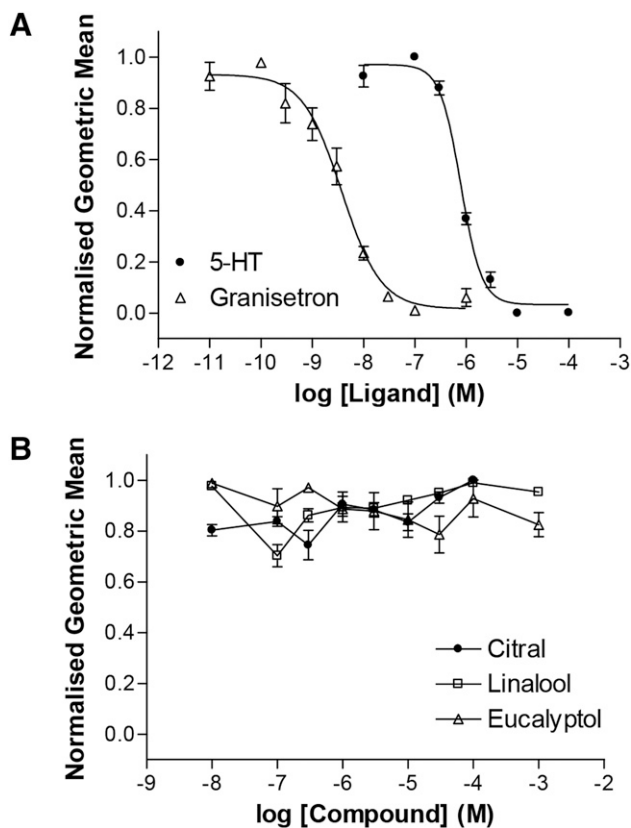
A

B

Fig. 5. Competition of a fluorescent 5-HT$_3$ receptor competitive antagonist. (A) Competition of 10 nM G-FL with the agonist 5-HT (pIC$_{50}$ = 6.10 ± 0.03, n_H = 2.1, IC$_{50}$ = 0.79 μM, n = 4) and the competitive antagonist granisetron (pIC$_{50}$ = 8.42 ± 0.03, n_H = 1.1, IC$_{50}$ = 3.8 nM, n = 6). (B) The test compounds citral (n = 3), eucalyptol (n = 3), and linalool (n = 3) show no competition with G-FL.

all data simultaneously (e.g., by incorporating both agonist concentration-activation and antagonist concentration-inhibition data), it generates a more comprehensive model of drug action and a statistically more powerful framework within which to evaluate specific hypotheses. This is particularly valuable when it is important to minimize use of resources, such as experimental animals or scarce test compounds.

Previously, we used a dual-application method to determine whether channel blockers have overlapping or independent binding sites within the 5-HT$_3$ receptor pore (Thompson et al., 2011b; Jarvis and Thompson, 2013). Results suggesting that bilobalide, ginkgolide B, and picrotoxinin shared binding sites and that diltiazem bound elsewhere were later confirmed by mutating channel-lining residues (Thompson et al., 2011a). Dual application of citral with bilobalide or diltiazem caused inhibition consistent with the allotopic model, indicating that citral binds at distinct sites to these two channel blockers. Eucalyptol and linalool caused dual inhibition at levels significantly greater than the syntopic predictions, indicating that these compounds also bind to distinct sites. However, dual inhibition exceeded the allotopic prediction, suggesting that eucalyptol and linalool may allosterically modulate binding of bilobalide and diltiazem. Alternatively, as the allotopic model assumes that the inhibitors do not modify the action of the agonist, it is possible that a reduced sensitivity to 5-HT could contribute to this effect, a possibility

that is supported by the rightward shift in the 5-HT EC$_{50}$ caused by eucalyptol.

The lipophilic nature of the oils suggests that the binding sites of citral, eucalyptol, and linalool are located in the transmembrane region, consistent with the slow wash-in and washout that is observed when compounds must first diffuse into membranes before reaching their target (Turina et al., 2006). This hypothesis is supported by our electrophysiology and flow cytometry data, which indicate a noncompetitive mechanism of action, and by the nonoverlapping binding sites predicted by our dual-application experiments. To probe for potential binding sites, we used homology modeling and docking, which predicted that all three oils share a common binding site located in a cavity between the transmembrane α-helices of adjacent subunits. The terpenoids carvacrol and thymol have been proposed to bind in a similar cavity within the 5-HT$_3$ receptor, and this location is also conserved among other Cys-loop receptors (Lansdell et al., 2015). Crystal structures of the invertebrate Cys-loop receptor glutamate-gated chloride channel reveal an equivalent intersubunit cavity occupied by ivermectin, and residues at this location are implicated in ivermectin binding at GABA$_A$ and glycine receptors (Lynagh and Lynch, 2012). A similar binding site has been identified for propofol at a prokaryotic homolog (*Gloeobacter* violaceus ligand-gated ion channel) and other eukaryotic Cys-loop receptors (Nury et al., 2011; Jayakar et al., 2013; Yip et al., 2013; Lynagh and Laube, 2014). The similar activities of these compounds across the Cys-loop receptor family suggest that this region is widely conserved and could be an amenable target for novel allosteric modulators (Corradi et al., 2011; Howard et al., 2011; Trattnig et al., 2012). To date, 5-HT$_3$ receptor antagonists have been typically used to prevent nausea and vomiting, but the association of these receptors with other disorders, such as irritable bowel syndrome, anxiety, and diabetic neuropathy, suggests that there may be scope for other therapeutic applications (Walstab et al., 2010; Silva et al., 2015).

The structurally related compounds carvacrol and thymol are also partial agonists at the 5-HT$_3$ receptor (Lansdell et al., 2015; Ziemba et al., 2015). As low-efficacy partial agonism can sometimes be overlooked and mistaken as antagonism [e.g., the 5-HT$_3$ ligand quipazine (Thompson and Lummis, 2013)], we tested citral, eucalyptol, and linalool for agonist activity using a 5-HT$_3$ receptor mutant with enhanced agonist sensitivity. Substitution of the 5-HT$_3$A subunit channel-lining 6' Thr with the equivalent 6' Ser from the 5-HT$_3$B subunit creates a hypersensitive mutant with increased sensitivity to a range of 5-HT$_3$ agonists (Thompson and Lummis, 2013). Consistent with previous reports, our results reveal a 2-fold increase in 5-HT sensitivity in the T6'S mutant. However—with citral, eucalyptol, and linalool—no agonist action, or potentiation of the 5-HT response, was observed at the mutant receptor, confirming that they are antagonists. In silico docking predicted that the 6' Thr residue may establish a hydrogen-bond interaction with linalool, although the interaction was with the backbone carbonyl and therefore unlikely to be greatly affected by amino acid substitution. Indeed, a 2-fold reduction in the potency of all the inhibitors at 5-HT$_3$A$_{T6'S}$ mutants suggests a nonspecific effect rather than a modification of hydrogen-bond interactions for linalool alone.
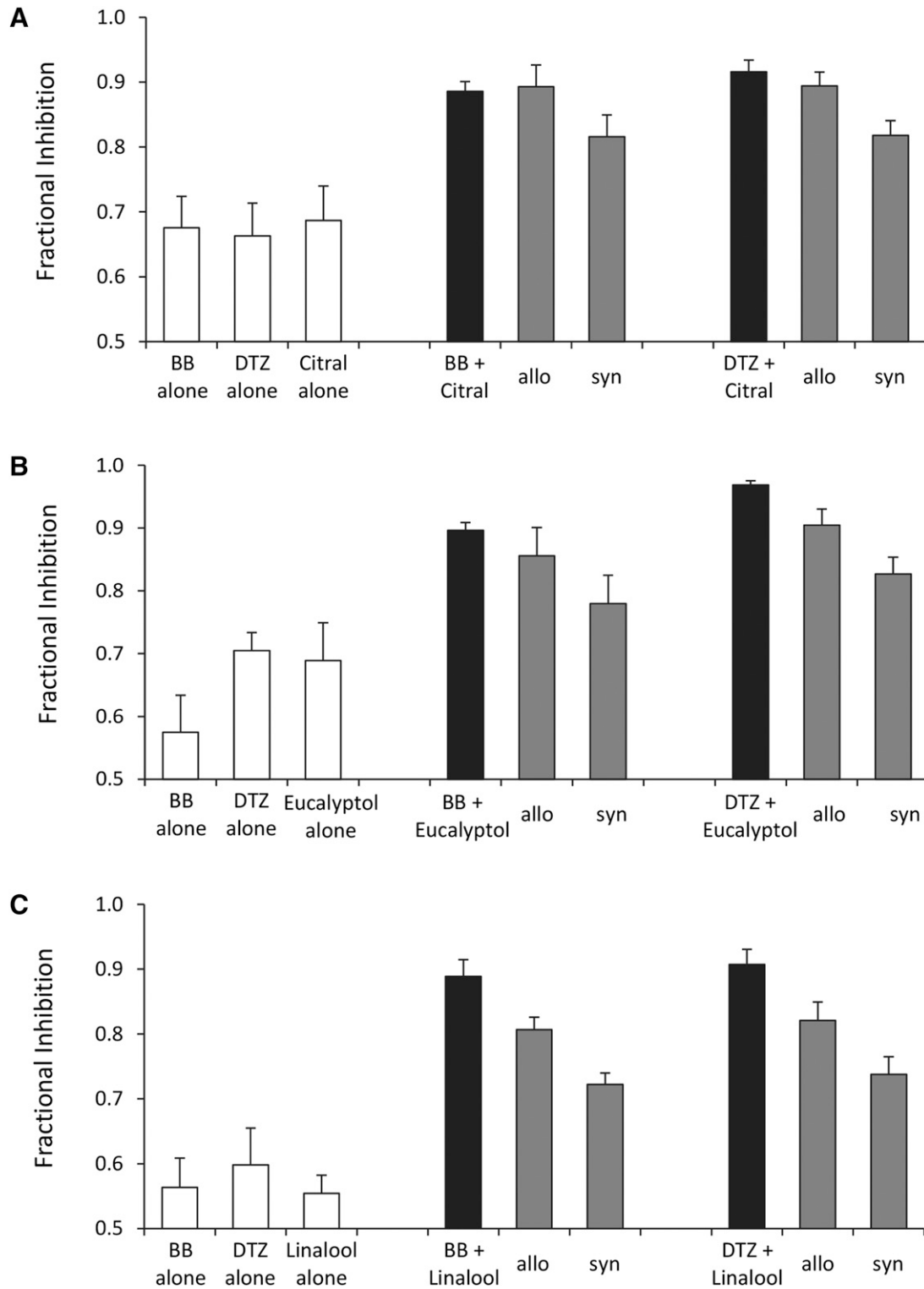
Fig. 6. Inhibition of the 5-HT$_3$ receptor using a dual-application approach. 5-HT$_3$ receptors were activated with a supramaximal (100 μM) concentration of 5-HT. Concentrations of BB, DTZ, and the terpenoids were preselected to inhibit the response by approximately 62% when used alone. Results are shown in the white bars. These same concentrations were then applied in dual combinations, giving results shown in the black bars. The gray bars are the allotopic (allo) and syntopic (syn) predictions based on the levels of inhibition caused by the compounds alone. Data are the mean ± S.E.M. Two-way analysis of variance with Dunnett's post-hoc test was used (IBM SPSS Statistics 20) to compare actual and predicted dual application responses. (A) Citral (n = 7). For BB, P = 0.019 (analysis of variance), P = 0.95 (H$_0$: BB+citral = allo), P = 0.031 (H$_0$: BB+citral = syn); and for DTZ, P = 0.0005 (analysis of variance), P = 0.42 (H$_0$: DTZ+citral = allo), P = 0.0004 (H$_0$: DTZ+citral = syn). (B) Eucalyptol (n = 6). For BB, P = 0.015 (analysis of variance), P = 0.38 (H$_0$: BB+eucalyptol = allo), P = 0.009 (H$_0$: BB+eucalyptol = syn); and for DTZ, P = 0.00008 (analysis of variance), P = 0.013 (H$_0$: DTZ+eucalyptol = allo), P = 0.00004 (H$_0$: DTZ+eucalyptol = syn). (C) Linalool (n = 5). For BB, P = 0.0006 (analysis of variance), P = 0.023 (H$_0$: BB+linalool = allo), P = 0.0004 (H$_0$: BB+linalool = syn); and for DTZ, P = 0.003 (analysis of variance), P = 0.056 (H$_0$: DTZ+linalool = allo), P = 0.002 (H$_0$: DTZ+linalool = syn). In all experiments, stable levels of inhibition were achieved by applying the compounds for 1 minute before 5-HT was added.
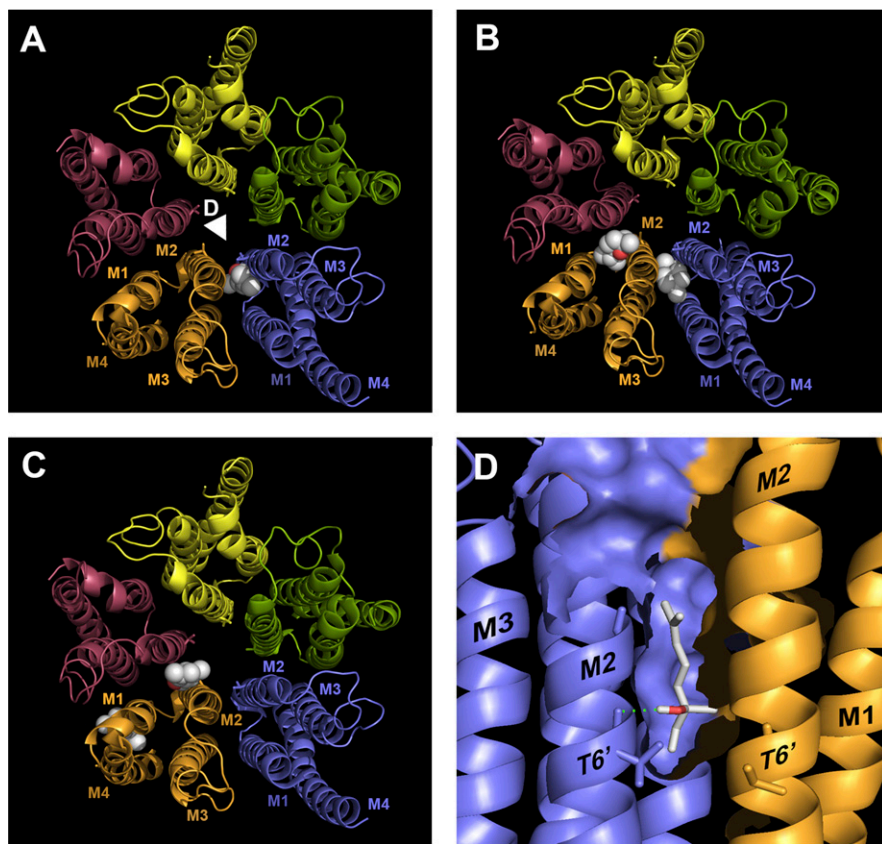
Fig. 7. Predicted binding locations for citral, eucalyptol, and linalool in a homology model of the human 5-HT$_3$ receptor. Using a loosely defined binding site (see *Materials and Methods*), 10 docked poses were generated for each ligand. Examples from the docked pose clusters (sphere representation) are shown at each of the predicted binding sites. The transmembrane domains of the five subunits that form the functional 5-HT$_3$ receptor are shown as different colored ribbons viewed from the extracellular side, with both the intracellular and extracellular domains removed for clarity. (A) A single binding site was predicted for linalool with the docked pose cluster differing by only 2.29 Å root-mean-square deviation. The white arrowhead indicates the origin from which (D) is viewed. (B) Two sites were predicted for eucalyptol, but were similarly located at the boundaries of adjacent subunits. (C) For citral, two potential binding sites were identified, a major (6/10) site at the interface of adjacent subunits and a minor site located at the lipid-exposed interface at the intracellular ends of M1 and M4. (D) In four of the 10 docked poses for linalool, PyMol 1.3 predicted hydrogen bonds (blue dotted line) between the ligand's terminal hydroxyl and the backbone of the channel-lining 6' Thr residue.

Several plant extracts are commonly used to treat gastrointestinal discomfort and respiratory disorders, and their components, such as citral and menthol, are reported to have relaxant effects on gut smooth muscle (Tangpu and Yadav, 2006; Hennebelle et al., 2008, Devi et al., 2011; Walstab et al., 2014). Here, we show that OELa, an extract from *L. alba*, inhibits 5-HT$_3$ receptors expressed in oocytes (IC$_{50}$ = 45 μg ml^{-1}) and 5-HT–evoked contractions in both rat trachea (IC$_{50}$ = 200 μg ml^{-1}) and guinea pig ileum (IC$_{50}$ = 20 μg ml^{-1}). Using LC-MS, we found the principal component of this oil was citral (75.9%), which could account for these effects; the IC$_{50}$ of OELa at expressed receptors is 45 μg ml^{-1}, which contains ~220 μM citral and is close to the IC$_{50}$ of citral alone (120 μM). It has been reported that 5-HT–mediated smooth muscle contractions in the trachea and ileum are partially regulated by 5-HT$_2$, 5-HT$_3$, and 5-HT$_4$ receptors. Our results with the antagonist granisetron confirm a role for 5-HT$_3$ receptors, similar to previous reports that used 5-HT$_3$ receptor antagonists to inhibit 5-HT–mediated smooth muscle contractions (Rocha e Silva et al., 1953; Tuladhar et al., 1997; Fernandez-Rodriguez et al., 2010; Kelley et al., 2014). Our results may therefore provide a mechanism for the medicinal use of these oils for relieving gastrointestinal and respiratory ailments. The IC$_{50}$ values we report here are comparable to those for similar terpenoid compounds, such as menthol (163 μM), and it has been suggested that oral administration of this compound could reach an equivalent concentration in vivo (Ashoor et al., 2013). However, to achieve this concentration in rat brain, the required intraperitoneal dose of menthol was 100 mg/kg, considerably higher than doses used for human medicinal products (Pan et al., 2012). Therefore, in humans, it is unlikely that systemic administration of typical doses would result in concentrations that are active at 5-HT$_3$ receptors, although it is possible that higher local concentrations following topical administration (e.g., in airway, skin, or gut) could reach pharmacologically active levels (Falk-Filipsson et al., 1993). For most terpenoids, including linalool and eucalyptol, blood and tissue concentrations have not been reported, but toxicological studies suggest that many are well tolerated (Oz et al., 2015). This suggests that there is still scope for therapeutic applications, with synthetic modification possibly providing a means for improving their potency and receptor selectivity.

In summary, we used nonlinear mixed-effects modeling to show that the oils citral, eucalyptol, and linalool inhibit homomeric 5-HT$_3$ receptors via noncompetitive mechanisms. Both electrophysiology and flow cytometry point to binding locations that do not overlap with the orthosteric binding site, whereas our dual-application experiments suggest actions that are mediated from outside the pore. Docking predicts a transmembrane binding site located between the α-helices of adjacent subunits, and is supported by the binding of related compounds to similar allosteric sites identified in both 5-HT$_3$ and other members of this ligand-gated ion channel family. These results demonstrate the value of analyzing data using nonlinear mixed-effects modeling and further highlight a conserved transmembrane binding site as a potential target for the development of novel allosteric ligands.
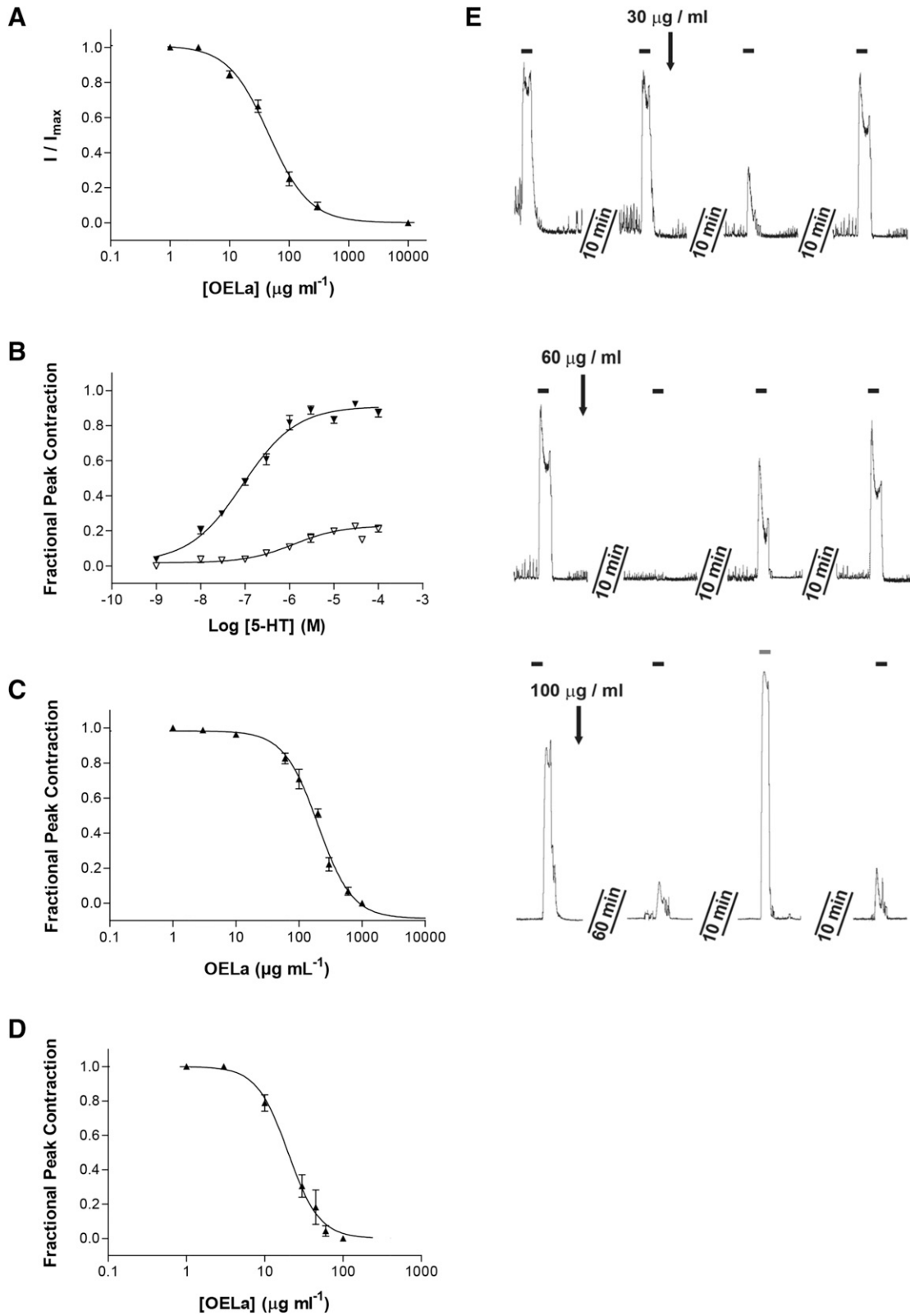
Fig. 8. The effects of OELa. (A) Concentration inhibition of 2 μM 5-HT–induced currents by OELa in *Xenopus* oocytes expressing the 5-HT₃ receptor (n = 5). (B) Rat tracheal contraction in response to 5-HT in the absence ($\blacktriangledown$, n = 6) and following a 10-minute preapplication with 10 μM granisetron ($\triangledown$, n = 3). (C) Concentration-inhibition of the 10 μM 5-HT–evoked tracheal contractile response by OELa (n = 4). (D) Inhibition by OELa of 10 μM 5-HT–evoked guinea pig ileum contractions (n = 6). (E). Example recordings from 5-HT–evoked (black bars) contractions of guinea pig ileum and their inhibition by 30, 60, and 100 μg ml^{-1} OELa. At concentrations ≥60 μg ml^{-1} OELa, the 5-HT–evoked contractions became increasingly slow to recover. Following a control 5-HT response (0.6 μM, black bar), the addition of 100 μg ml^{-1} OELa continued to inhibit the 5-HT–evoked contractions 50 minutes later, although an acetylcholine (1 μM, gray bar) response was unaltered. Parameters defining the curves are shown in the text.

Switzerland) for reviewing the chemical structures and providing G-FL, and Ruth Murrell-Lagnado for hosting the experimental work.

References

Abdel-Aziz H, Windeck T, Ploch M, and Verspohl EJ (2006) Mode of action of gingerols and shogaols on 5-HT$_3$ receptors: binding studies, cation uptake by the receptor channel and contraction of isolated guinea-pig ileum. *Eur J Pharmacol* **530**:136–143.

Ashoor A, Nordman JC, Veltri D, Yang KH, Shuba Y, Al Kury L, Sadek B, Howarth FC, Shehu A, and Kabbani N, et al. (2013) Menthol inhibits 5-HT$_3$ receptor-mediated currents. *J Pharmacol Exp Ther* **347**:398–409.

Barann M, Dilger JP, Bönisch M, Göthert M, Dybek A, and Urban BW (2000) Inhibition of 5-HT$_3$ receptors by propofol: equilibrium and kinetic measurements. *Neuropharmacology* **39**:1064–1074.

Caputi L and Aprea E (2011) Use of terpenoids as natural flavouring compounds in food industry. *Recent Pat Food Nutr Agric* **3**:9–16.

Chiara DC, Jayakar SS, Zhou X, Zhang X, Savechenkov PY, Bruzik KS, Miller KW, and Cohen JB (2013) Specificity of intersubunit general anesthetic-binding sites in the transmembrane domain of the human $\alpha1\beta3\gamma2$ γ-aminobutyric acid type A (GABAA) receptor. *J Biol Chem* **288**:19343–19357.

Colquhoun D (2007) Why the Schild method is better than Schild realised. *Trends Pharmacol Sci* **28**:608–614.

Corradi J, Andersen N, and Bouzat C (2011) A novel mechanism of modulation of 5-HT3A receptors by hydrocortisone. *Biophys J* **100**:42–51.

Devi RC, Sim SM, and Ismail R (2011) Spasmolytic effect of citral and extracts of *Cymbopogon citratus* on isolated rabbit ileum. *J Smooth Muscle Res* **47**:143–156.

Falk-Filipsson A, Löf A, Hagberg M, Hjelm EW, and Wang Z (1993) d-limonene exposure to humans by inhalation: uptake, distribution, elimination, and effects on the pulmonary function. *J Toxicol Environ Health* **38**:77–88.

Fernandez-Rodriguez S, Broadley KJ, Ford WR, and Kidd EJ (2010) Increased muscarinic receptor activity of airway smooth muscle isolated from a mouse model of allergic asthma. *Pulm Pharmacol Ther* **23**:300–307.

García DA, Bujons J, Vale C, and Suñol C (2006) Allosteric positive interaction of thymol with the GABA$_A$ receptor in primary cultures of mouse cortical neurons. *Neuropharmacology* **50**:25–35.

Hales TG and Lambert JJ (1991) The actions of propofol on inhibitory amino acid receptors of bovine adrenomedullary chromaffin cells and rodent central neurones. *Br J Pharmacol* **104**:619–628.

Hall AC, Turcotte CM, Betts BA, Yeung WY, Agyeman AS, and Burk LA (2004) Modulation of human GABA$_A$ and glycine receptor currents by menthol and related monoterpenoids. *Eur J Pharmacol* **506**:9–16.

Hassaine G, Deluz C, Grasso L, Wyss R, Tol MB, Hovius R, Graff A, Stahlberg H, Tomizaki T, Desmyter A, Moreau C, Li XD, Poitevin F, Vogel H, and Nury H (2014) X-ray structure of the mouse serotonin 5-HT$_3$ receptor. *Nature* **512**:276–281.

Hawthorne R, Cromer BA, Ng HL, Parker MW, and Lynch JW (2006) Molecular determinants of ginkgolide binding in the glycine receptor pore. *J Neurochem* **98**:395–407.

Heimes K, Hauk F, and Verspohl EJ (2011) Mode of action of peppermint oil and (-)-menthol with respect to 5-HT$_3$ receptor subtypes: binding studies, cation uptake by receptor channels and contraction of isolated rat ileum. *Phytother Res* **25**:702–708.

Hennebelle T, Sahpaz S, Joseph H, and Bailleul F (2008) Ethnopharmacology of *Lippia alba*. *J Ethnopharmacol* **116**:211–222.

Howard RJ, Murail S, Ondricek KE, Corringer PJ, Lindahl E, Trudell JR, and Harris RA (2011) Structural basis for alcohol modulation of a pentameric ligand-gated ion channel. *Proc Natl Acad Sci USA* **108**:12149–12154.

Sali A and Blundell TL (1993) Comparative protein modelling by satisfaction of spatial restraints. *J Mol Biol* **234**:779–815.

Jack J, Simonin J, Ruepp MD, Thompson AJ, Gertsch J, and Lochner M (2015) Characterizing new fluorescent tools for studying 5-HT$_3$ receptor pharmacology. *Neuropharmacology* **90**:63–73.

Jarvis GE and Thompson AJ (2013) A golden approach to ion channel inhibition. *Trends Pharmacol Sci* **34**:481–488.

Jayakar SS, Dailey WP, Eckenhoff RG, and Cohen JB (2013) Identification of propofol binding sites in a nicotinic acetylcholine receptor with a photoreactive propofol analog. *J Biol Chem* **288**:6178–6189.

Kelley SP, Walsh J, Kelly MC, Muhdar S, Adel-Aziz M, Barrett ID, and Wildman SS (2014) Inhibition of native 5-HT3 receptor-evoked contractions in guinea pig and mouse ileum by antimalarial drugs. *Eur J Pharmacol* **738**:186–191.

Kessler A, Sahin-Nadeem H, Lummis SC, Weigel I, Pischetsrieder M, Buettner A, and Villmann C (2014) GABA$_{(A)}$ receptor modulation by terpenoids from Sideritis extracts. *Mol Nutr Food Res* **58**:851–862.

Kesters D, Thompson AJ, Brams M, van Elk R, Spurny R, Geitmann M, Villalgordo JM, Guskov A, Danielson UH, and Lummis SC, et al. (2013) Structural basis of ligand recognition in 5-HT$_3$ receptors. *EMBO Rep* **14**:49–56.

Lansdell SJ, Sathyaprakash C, Doward A, and Millar NS (2015) Activation of human 5-hydroxytryptamine type 3 receptors via an allosteric transmembrane site. *Mol Pharmacol* **87**:87–95.

Lynagh T and Laube B (2014) Opposing effects of the anesthetic propofol at pentameric ligand-gated ion channels mediated by a common site. *J Neurosci* **34**:2155–2159.

Lynagh T and Lynch JW (2012) Ivermectin binding sites in human and invertebrate Cys-loop receptors. *Trends Pharmacol Sci* **33**:432–441.

McWilliam H, Li W, Uludag M, Squizzato S, Park YM, Buso N, Cowley AP, and Lopez R (2013) Analysis Tool Web Services from the EMBL-EBI. *Nucleic Acids Res* **41**:W597–W600.

Moore NA, Sargent BJ, Manning DD, and Guzzo PR (2013) Partial agonism of 5-HT$_3$ receptors: a novel approach to the symptomatic treatment of IBS-D. *ACS Chem Neurosci* **4**:43–47.

Mould DR and Upton RN (2013) Basic concepts in population modeling, simulation, and model-based drug development-part 2: introduction to pharmacokinetic modeling methods. *CPT Pharmacometrics Syst Pharmacol* **2**:e38.

Nury H, Van Renterghem C, Weng Y, Tran A, Baaden M, Dufresne V, Changeux JP, Sonner JM, Delarue M, and Corringer PJ (2011) X-ray structures of general anaesthetics bound to a pentameric ligand-gated ion channel. *Nature* **469**:428–431.

Oz M, Lozon Y, Sultan A, Yang KH, and Galadari S (2015) Effects of monoterpenes on ion channels of excitable cells. *Pharmacol Ther* **152**:83–97.

Pan R, Tian Y, Gao R, Li H, Zhao X, Barrett JE, and Hu H (2012) Central mechanisms of menthol-induced analgesia. *J Pharmacol Exp Ther* **343**:661–672.

Rocha e Silva M, Valle JR, and Picarelli P (1953) A pharmacological analysis of the mode of action of serotonin (5-hydroxytryptamine) upon the guinea-pig ileum. *Br J Pharmacol* **8**:378–388.

Silva M, Martins D, Tavares I, and Morgado C (2015) Inhibition of spinal 5-HT$_3$R reverted diabetes-induced mechanical hypersensitivity in a GABA$_A$R-mediated neurotransmission-dependent manner. *Neuroscience* **304**:228–239.

Spalding MD and Jarvis GE (2002) The impact of the 1998 coral mortality on reef fish communities in the Seychelles. *Mar Pollut Bull* **44**:309–321.

Tangpu V and Yadav AK (2006) Antidiarrhoeal activity of Cymbopogon citratus and its main constituent, citral. *Pharmacologyonline* **2**:290–298.

Thompson AJ, Duke RK, and Lummis SC (2011a) Binding sites for bilobalide, diltiazem, ginkgolide, and picrotoxinin at the 5-HT$_3$ receptor. *Mol Pharmacol* **80**:183–190.

Thompson AJ, Jarvis GE, Duke RK, Johnston GA, and Lummis SC (2011b) Ginkgolide B and bilobalide block the pore of the 5-HT3receptor at a location that overlaps the picrotoxin binding site. *Neuropharmacology* **60**:488–495.

Thompson AJ, Lester HA, and Lummis SC (2010) The structural basis of function in Cys-loop receptors. *Q Rev Biophys* **43**:449–499.

Thompson AJ and Lummis SC (2013) A single channel mutation alters agonist efficacy at 5-HT3A and 5-HT3AB receptors. *Br J Pharmacol* **170**:391–402.

Trattnig SM, Harpsøe K, Thygesen SB, Rahr LM, Ahring PK, Balle T, and Jensen AA (2012) Discovery of a novel allosteric modulator of 5-HT$_3$ receptors: inhibition and potentiation of Cys-loop receptor signaling through a conserved transmembrane intersubunit site. *J Biol Chem* **287**:25241–25254.

Tuladhar BR, Kaisar M, and Naylor RJ (1997) Evidence for a 5-HT$_3$ receptor involvement in the facilitation of peristalsis on mucosal application of 5-HT in the guinea pig isolated ileum. *Br J Pharmacol* **122**:1174–1178.

Turina AV, Nolan MV, Zygadlo JA, and Perillo MA (2006) Natural terpenes: self-assembly and membrane partitioning. *Biophys Chem* **122**:101–113.

Walstab J, Krüger D, Stark T, Hofmann T, Demir IE, Ceyhan GO, Feistel B, Schemann M, and Niesler B (2013) Ginger and its pungent constituents non-competitively inhibit activation of human recombinant and native 5-HT$_3$ receptors of enteric neurons. *Neurogastroenterol Motil* **25**:439–447, e302.

Walstab J, Rappold G, and Niesler B (2010) 5-HT$_{(3)}$ receptors: role in disease and target of drugs. *Pharmacol Ther* **128**:146–169.

Walstab J, Wohlfarth C, Hovius R, Schmitteckert S, Röth R, Lasitschka F, Wink M, Bönisch H, and Niesler B (2014) Natural compounds boldine and menthol are antagonists of human 5-HT$_3$ receptors: implications for treating gastrointestinal disorders. *Neurogastroenterol Motil* **26**:810–820.

Yip GM, Chen ZW, Edge CJ, Smith EH, Dickinson R, Hohenester E, Townsend RR, Fuchs K, Sieghart W, and Evers AS, et al. (2013) A propofol binding site on mammalian GABA$_A$ receptors identified by photolabeling. *Nat Chem Biol* **9**:715–720.

Ziemba PM, Schreiner BS, Flegel C, Herbrechter R, Stark TD, Hofmann T, Hatt H, Werner M, and Gisselmann G (2015) Activation and modulation of recombinantly expressed serotonin receptor type 3A by terpenes and pungent substances. *Biochem Biophys Res Commun* **467**:1090–1096.

Address correspondence to: Dr. Andrew J. Thompson, Department of Pharmacology, Tennis Court Road, Cambridge CB2 1PD. E-mail: ajt44@cam.ac.uk